

Time-dependent seismicity analysis in the Northwest Himalaya and its adjoining regions

P. Chingtham¹ · R. B. S. Yadav² · S. Chopra³ ·
Arabind Kumar Yadav⁴ · A. K. Gupta¹ · P. N. S. Roy⁵

Received: 19 September 2014 / Accepted: 11 October 2015 / Published online: 22 October 2015
© Springer Science+Business Media Dordrecht 2015

Abstract The Northwest Himalaya and its adjoining regions are one of the most seismically vulnerable regions in the Indian subcontinent which have experienced two great earthquakes [1902 Caucasus of magnitude M_S 8.6 and 1905 Kangra, India of M_S 8.6 (M_W 7.8)] and several large damaging earthquakes in the previous century. In this study, time-dependent seismicity analysis is carried out in five main seismogenic zones in the Northwest Himalaya and its adjoining regions by considering earthquake inter-arrival times using a homogeneous and complete earthquake catalogue for the period 1900–2010 prepared by Yadav et al. (Pure Appl Geophys 169:1619–1639, 2012a). For this purpose, we consider three statistical models, namely Poisson (time independent), Lognormal and Weibull (time dependent). Fitness of inter-arrival time data is investigated using Kolmogorov–Smirnov (K–S) test for Lognormal and Weibull models, while Chi-square test is applied for the Poisson model. It is observed that the Lognormal model fits remarkably well to the observed inter-arrival time data, while the Weibull model exhibits moderate fitting. The parameters A and B of the time-dependent seismicity equation $\ln IAT = A + BM \pm C$ (where $\ln IAT$ is the log of inter-arrival times of earthquakes exceeding magnitude M and C is the standard deviation), developed by Musson et al. (Bull Seismol Soc Am 92:1783–1794, 2002) are evaluated in each of the five main seismogenic zones considered in the region. The mean of the inter-arrival times for the Lognormal distribution is found to be linearly related to the lower-bound magnitude (M_{\min}). Values of the slope (B) of the mean vary from 2.34 to 2.57, while the parameter A ranges from -9.06 to -7.01 in the examined seismogenic zones with standard deviation ranging from 0.21 to 0.38. It is observed that the Hindukush–Pamir

✉ R. B. S. Yadav
rbsybhu@rediffmail.com; rbsykuk@gmail.com

¹ National Center for Seismology, Ministry of Earth Sciences, New Delhi, India

² Department of Geophysics, Kurukshetra University, Kurukshetra, Haryana 136119, India

³ Institute of Seismological Research (ISR), Gandhinagar, Gujarat, India

⁴ Department of Geology and Geophysics, Indian Institute of Technology, Kharagpur, India

⁵ Department of Applied Geophysics, Indian School of Mines, Dhanbad, India

Himalaya and Himalayan Frontal Thrust exhibit higher seismic hazard (i.e., high seismic activity and low recurrence periods), while the Sulaiman–Kirthar ranges show the lowest. The variation in estimated seismicity parameters from one zone to another reveals high crustal heterogeneity and seismotectonic complexity in the study region.

Keywords Time-dependent model · Recurrence periods · Lognormal model · Poisson model · Gutenberg–Richter (G–R) relation

1 Introduction

Earthquakes have long been understood to occur randomly in time, space and magnitude. It is a general hypothesis that the earthquakes form a stochastically independent sequence of events in time and space. Therefore, the earthquake occurrences can be modeled as a Poisson process (time independent). The Poisson model assumes that the recurrence time of an earthquake follows the Poisson distribution, where the probability of recurrence of an earthquake event is independent of the time elapsed since the last event. The Poisson process has been used extensively in the probabilistic seismic hazard analysis by a number of researchers all around the globe. Small and medium magnitude earthquakes may occur independently implying a Poisson distribution of earthquake occurrences. However, studies by various authors (i.e., Kagan and Knopoff 1976; Kagan and Jackson 1991; Knopoff et al. 1996) imply clustering in time for large earthquakes and hence proposed other type of distributions. Moreover, elastic rebound theory (Reid 1911) suggests that occurrences of earthquakes on a particular fault or seismic zone are not independent from each other. It has been observed that release of accumulated stress in a fault or seismic zone and the occurrence of an earthquake reduce the probability for occurrence of a following independent earthquake at the same fault/fault segment or seismic zone. Time-dependent recurrence models assume that there is a dependence of the probability of recurrence and time elapsed since the last earthquake.

Inter-arrival time and magnitude of the successive earthquakes are one of the important challenges to forecast for the seismological community in the world. Inter-arrival times are the time intervals between the events on all the faults in a particular region, while recurrence times are the time intervals between the events on a single fault/fault segment. The time- and space-dependent models exhibit very different hazard estimates from the Poisson model, depending on the duration of the gap (i.e., the elapsed time since the last event) and the average inter-arrival time. It has been observed by Anagnos and Kiremidjian (1988) that the time-dependent models predict a considerably greater hazard than the Poisson model, since the time elapsed from the last major earthquake is of the order of the mean inter-arrival times.

Several earthquake generation (time-independent and time-dependent) models (Poisson, double Poisson, Markov, semi-Markov, regenerative point process, renewal process, Weibull, Gamma, Lognormal, exponential, Brownian Passage-Time (BPT) and among others) have been extensively used by various researchers for earthquake hazard assessment in different regions of the world. A number of researchers (e.g., Gardner and Knopoff 1974; Kijko and Sellevoll 1989, 1992; Kijko 2004 among others) studied the Poisson distribution for earthquakes which shows the time-independent behavior of larger magnitude earthquake occurrences. However, several studies of larger earthquakes show temporal dependence of earthquakes in several regions of the world (Bufe et al. 1977;

Sykes and Quittmeyer 1981; Papazachos 1989; Kagan and Jackson 1991; Papadimitriou and Papazachos 1994; Tsapanos and Papazachos 1994; Papazachos et al. 1994; Knopoff et al. 1996; Yadav et al. 2008, 2010a). A number of studies have been carried out on time-predictable recurrence model for large earthquakes along the plate boundaries (Bufe et al. 1977; Shimazaki and Nakata 1980; Sykes and Quittmeyer 1981). Bufe et al. (1977) suggested a seismic slip and recurrence interval model for a segment of a fault in northern California and observed that the time interval is proportional to the amount of displacement in the preceding earthquake. Shimazaki and Nakata (1980) observed that for a larger earthquake there is a longer following quiet period for the sequences of large thrust fault earthquakes in Japan. Sykes and Quittmeyer (1981) observed that the repeat times of large earthquakes agree better with the time-predictable model. Sornette and Knopoff (1997) reviewed a number of possible statistical distributions and concluded that those distributions which decay more slowly than exponential are better. Davis et al. (1989) proposed that the Lognormal distribution for inter-event times describes vividly the earthquake occurrences by considering the assumption that the probability of the next earthquake increases with the increasing of the elapsed time of the last earthquake. Ward and Goes (1993) and Goes and Ward (1994) suggested that earthquake occurrences can be best explained by the Weibull distribution depending on the exponent in the distribution. A regional time- and magnitude-predictable model was proposed by Papazachos (1989, 1992), which was further modified by Papazachos and Papaioannou (1993) and applied in the seismogenic zones of the Aegean and its surrounding regions. This model was tested in several regions of the world by several researchers. Musson et al. (2002) developed a new time-dependent seismicity model for the estimation of inter-arrival times of larger earthquakes in Japan and Greece regions. This model appears similar to the Gutenberg–Richter (G–R) magnitude–frequency recurrence relation, but more informative than the G–R relation. Time-dependent seismic hazard in the Indian subcontinent has been assessed by a number of researchers using several statistical models (e.g., Parvez and Ram 1997, 1999; Tripathi 2006; Yadav et al. 2008, 2010a, b among others).

In this study, we aim to investigate the inter-occurrence time statistics in the Northwest Himalaya and its adjoining regions following Musson et al. (2002) time-dependent model, using a homogeneous and complete earthquake catalogue during the period 1900–2010 prepared by Yadav et al. (2012a). This analysis is performed in the five main seismogenic zones in the study region that was delineated by Yadav et al. (2013a). The time-dependent probabilities and seismicity parameters of this model in these zones are described using the Lognormal distribution.

2 Seismotectonics of the study region

Geographically, the study region is bounded by 25°–40°N and 65°–85°E and located in the Himalayan part of Alpide belt and its neighboring regions which include India, Pakistan, Afghanistan, Hindukush, Pamirs, Mangolia and Tien–Shan (Fig. 1). This region is one of the most seismically active continent–continent (Indian–Eurasian plates) collision-type active plate margin regions of the world and situated at the western syntaxis of the Himalaya. Structurally, this region is controlled by large rigid lithospheric blocks of the Indian plate from the south, the Afghan block in the southwest, the Turan plate in the west and the Tarim block in the northeast (Koulakov and Sobolev 2006; Yadav 2009; Yadav et al. 2012a). The region exhibits intensive folding and thrusting, which occurred in the

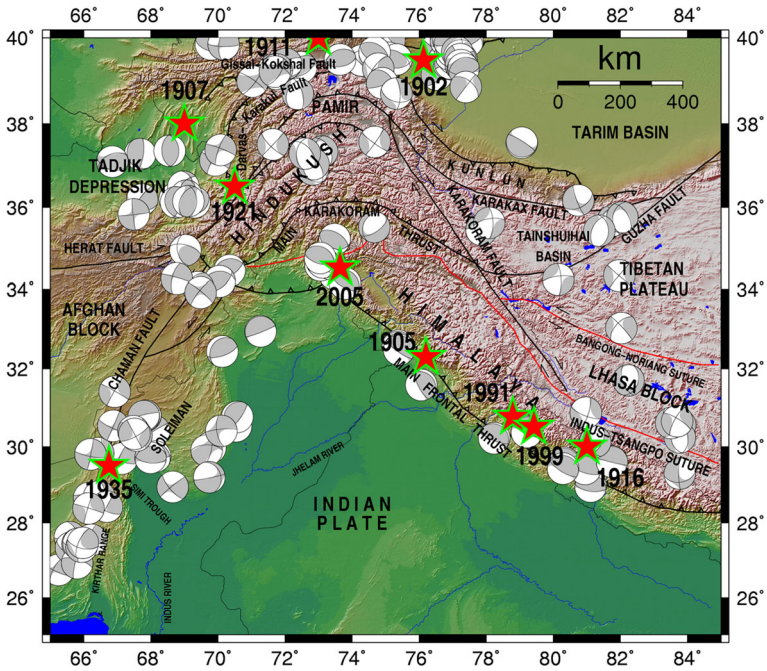


Fig. 1 Tectonic and geomorphological map showing the fault and fold systems in the Hindukush–Pamir Himalaya and adjoining region (after Koulakov and Sobolev 2006; Yadav 2009; Yadav et al. 2010a). Focal mechanism solutions of shallow earthquakes $M_w \geq 5.5$ obtained by Harvard GCMT catalogue during 1976–2010 are also shown with gray color beach ball in the map revealing the style of faulting in different parts of the region

Cenozoic and Mesozoic era (Gansser 1964). The trend of folding and faulting in the Himalayan region is NW–SE to EW direction. Toward north of the Pamir region, there is no well-defined tectonic belt. The Main Himalayan Frontal Thrust (HFT) and the Hazara, Sulaiman and Kirthar ranges highlight the collisional deformations of the Indian and Eurasian plates (Chingtham et al. 2013; Seeber and Armbruster 1981; Thingbaijam et al. 2009; Yadav et al. 2012a, 2015).

Two great earthquakes (1902 Caucasus (M_S 8.6) and 1905 Kangra, India (M_S 8.6, M_w 7.8) and several moderate-to-large earthquakes have occurred during previous century in this region (Gutenberg and Richter 1954). Several researchers (e.g., Chatelain et al. 1980; Burtman and Molnar 1993; Fan et al. 1994; Arora et al. 2012) suggested that two converging seismic regimes—northward subduction of the Indian plate beneath the Hindukush and southward subduction of the Eurasian plate below the Pamir—control the seismicity of the Hindukush–Pamir thrust zone. The western part of the Himalayan arc, consisting of the Kashmir ranges, turns to the south near Nanga Parbat to form the Hazara syntaxis (Meltzer et al. 2001), where the 2005 Kashmir earthquake (M_w 7.6) was nucleated. Other major faults such as Chaman, Herat, Ornach-Nal and Karakoram are believed to be slip-transacts. The Chaman fault zone has been associated with two major earthquakes: 1931, Mach (M_S 7.4, M_w 7.1) and 1945 (M_w 7.7) Quetta. The Arabian plate is apparently being subducted northward, forming the subduction zone overlying the E–W-trending Makran ranges (Quittmeyer and Jacob 1979). The seismogenic surge of the 1945 Makran (M_w 8.1)

earthquake triggered a tsunami in Pakistan and Indian regions. In recent past, the Himalayan Frontal Thrust belt of the Indian region has experienced three moderate-to-large earthquakes of M_W 6.8 and 6.5 in 1991 and 1999 at Uttarkashi and Chamoli regions, respectively, and most devastating earthquake of the Kashmir Himalaya in 2005 of M_W 7.6 (Fig. 1).

3 The earthquake catalogue and delineation of seismogenic zones

Earthquake catalogue should be accurate, homogeneous and complete in space and time. Yadav et al. (2012a) compiled a homogeneous and complete earthquake catalogue for the studied region using various historical (Tandon and Srivastava 1974; Chandra 1978; Bapat et al. 1983; Oldham 1883) and instrumental earthquake data (ISC, since 1964; <http://www.isc.ac.uk/search/bulletin>; the NEIC, since 1963; <http://neic.usgs.gov/neis/epic/epic-global.htm> and the HRVD, since 1976; now operated as the Global Centroid-Moment-Tensor project at Lamont-Doherty Earth Observatory (LDEO) of Columbia University; <http://www.globalcmt.org/CMTsearch.html>). This catalogue has been homogenized for the moment magnitude scale (M_W) using different established empirical regression relationships among different magnitude scales (Yadav et al. 2012a). The prepared catalogue was also cleaned for dependent events (foreshocks and aftershocks) using Uhrhammer (1986) spatial and temporal windowing methods. The completeness of earthquake catalogue has been performed with respect to magnitude and time. A visual cumulative method given by Mulargia and Tinti (1985) is used to check the completeness with respect to time. On this basis, subcatalogue is then segregated into complete and incomplete subcatalogues. The completeness of the catalogue with time for various magnitude thresholds is listed in Table 1. A complete procedure for compilation and completeness analysis of this catalogue is provided by Yadav et al. (2012a). Considering only the complete part of the subcatalogue, we estimated the inter-arrival times for magnitude ranging from M_W 4.0 to the largest event occurring at least twice.

In order to investigate the time-dependent seismicity in the studied region, we used homogenous and complete earthquake catalogue consisting of 9250 events with $M_W \geq 4.0$ for the period 1900–2010. The time-dependent seismicity analysis has been performed in certain seismogenic zones in the studied region. Five main seismogenic source zones (Fig. 2), used in this study, are defined and delineated by Yadav et al. (2013a). These seismic source zones have been delineated using three fundamental characteristics, namely past seismic history, tectonics and focal mechanism of earthquake of magnitude greater than M_W 5.0. These seismogenic source zones are the Sulaiman–Kirthar ranges (Zone 1), Northern Pakistan and Hazara syntaxis (Zone 2), Hindukush–Pamir Himalayas (Zone 3), Himalayan Frontal Thrusts (Zone 4) and Tibetan Plateau (Zone 5). If we consider the

Table 1 The completeness period estimated from visual cumulative method for different threshold magnitudes of the earthquake catalogue used

Sl.no.	Magnitude class	Completeness time period
1	$M_W \geq 4.0$	1975–2010
2	$M_W \geq 4.5$	1965–2010
3	$M_W \geq 5.0$	1960–2010
4	$M_W \geq 5.5$	1920–2010
5	$M_W \geq 6.0$	1900–2010

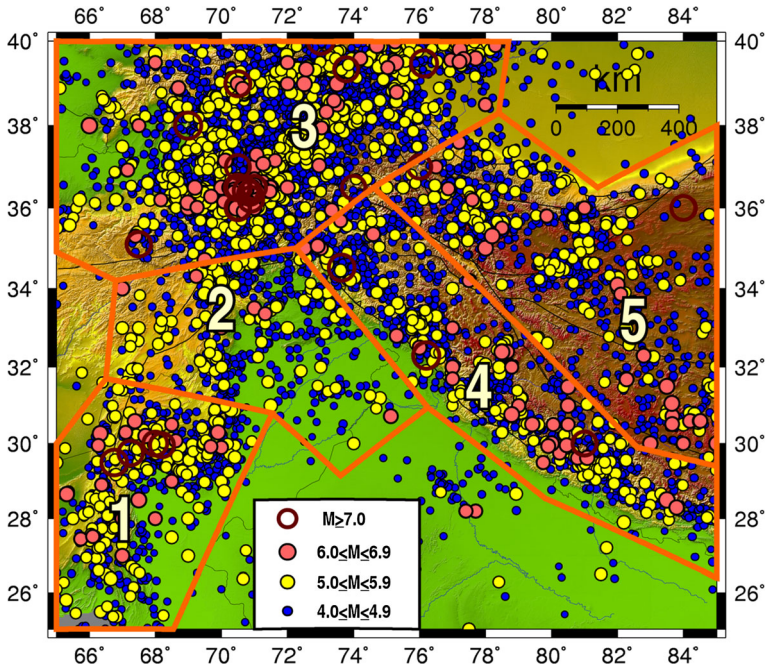


Fig. 2 Delineation of five broad seismicogenic source zones in the Northwest frontier of the Himalayas on the basis of seismicity, tectonics and focal mechanism of earthquakes. The epicentral distribution of independent earthquakes (mainshocks) of $M_W \geq 4.0$ occurred during the period 1900–2010 is also shown in the figure along with source zones that reveals seismic activity of each zone (modified after Yadav et al. 2013a)

depth-wise variation in seismicity, Zone 3 (Hindukush–Pamir Himalaya) can further be divided into two parts, i.e., shallow ($h < 70$ km) and intermediate-depth seismicity ($h \geq 70$ km) zones. The details of these main seismicogenic zones can be found in Yadav et al. (2013a). These seismicogenic source zones, used in this study, are shown in Fig. 2 along with the seismicity ($M_W \geq 4.0$ during 1900–2010) of the region.

4 Time-dependent seismic hazard model

The general accepted practice in the seismic hazard studies is to consider occurrences of earthquakes to be Poissonian in time-independent approach. The recent developments in seismic hazard assessment have incorporated the time-dependent earthquake recurrence model (i.e., renewal model) which is considered to be an important component in the modern-day Probabilistic Seismic Hazard Analysis (PSHA) (e.g., Working Group on California Earthquake Probabilities WGCEP 1995; Kumamoto 1999; Cramer et al. 2000; Papaioannou and Papazachos 2000; Frankel et al. 2002; Peruzza and Pace 2002; WGCEP 2003; Erdik et al. 2004; Pace et al. 2006; Petersen et al. 2007, 2008). In time-dependent probabilistic seismic hazard analysis, the inter-arrival time is an important parameter which is calculated by various methods: relation between displacement during the event and the slip rate on the fault, paleoseismicity analysis or from historical catalogue. In order to estimate inter-arrival from historical catalogue, the time span of the catalogue needs to

be at least twice of the inter-arrival time of the magnitude. Relationship between inter-arrival time and magnitude can be used to estimate the inter-arrival time for different magnitudes. There are number of models proposed to include the time dependence of the source model. Musson et al. (2002) suggested that the seismicity can be assessed by a time-predictable model given by the following statistical equation:

$$\ln \text{IAT} = A + BM \pm C \quad (1)$$

where IAT shows the inter-arrival times between two successive earthquakes of magnitude M or larger. The parameters A , B and C are regional constants. The parameter C represents the standard deviation.

4.1 Computation of inter-arrival times

Inter-arrival time (IAT) is computed for magnitude M , ranging from the minimum magnitude of the catalogue completeness ($M_W = 4.0$) to the maximum magnitude occurring at least twice in the catalogue. All the earthquakes of magnitude greater than or equal to M have been employed to compute the inter-arrival time at M . In the present analysis, M represents the homogenized moment magnitude M_W .

4.2 Model fitting between inter-arrival time (IAT) and magnitude

The inter-arrival times calculated above are fitted to the Lognormal, Poisson and Weibull models. We examined fitness of the inter-arrival times data with Lognormal and Weibull distributions using standard Kolmogorov–Smirnov (K–S) test, while for Poisson distribution, the Chi-square test is employed with the maximum likelihood estimator of the parameter. The reason behind pursuing different tests can be vividly explained by different types of the distributions, viz for continuous distributions, K–S is the commonly used test, while for discrete distributions, such as the Poisson, Chi-square test is commonly applied (Musson et al. 2002).

The best model was selected using fitness test applied with respect to the variation in inter-arrival times with magnitude in all seismogenic zones.

4.3 Computation of model parameters

We computed the inter-arrival times (IAT) for the earthquake of magnitude M , where M is varying from minimum magnitude $M_W = 4.0$ to the maximum magnitude occurring at least twice in each of the seismogenic zone. Deeper events, considered here to be greater than 70 km focal depth in the Hindukush and Pamir Himalaya and adjoining regions, were excluded while computing the earthquake inter-arrival times keeping in mind that deeper events do not contribute more in the seismic hazard. The variation in the IAT with magnitude is fitted through three models, namely Lognormal, Poisson and Weibull. The sets of inter-arrival times were, then, analyzed to inspect the goodness of fit to three different types of model, namely Lognormal, Poisson and Weibull for each of the five main zones as depicted in Figs. 3a, 4, 5, 6 and 7a. Figures 3a, 4, 5, 6 and 7a depict the distribution of different models with respect to the observed inter-arrival times. The results of calculated p value of different tests in each of the five zones are shown in Tables 2, 3 and 4. On the basis of standard decision rule, the model can be proclaimed as fit to the

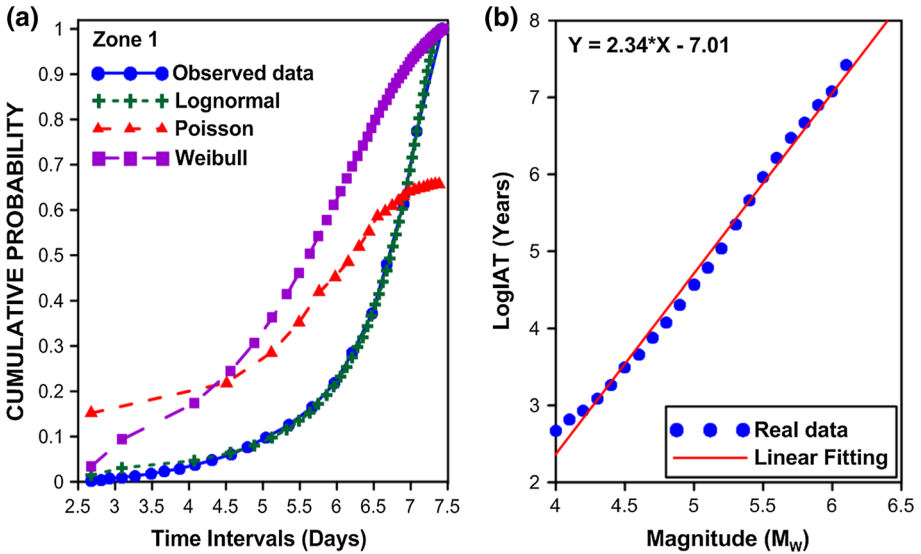


Fig. 3 a Cumulative plots of the distribution of log inter-arrival times for Zone 1. The x and y axes represent the log of inter-arrival times and the cumulative probability, respectively. The three different distributions, i.e., Lognormal, Weibull and Poisson shown by *different lines* are plotted to check the fitness with the observed data. b Plot of log inter-arrival times against magnitudes for Zone 1

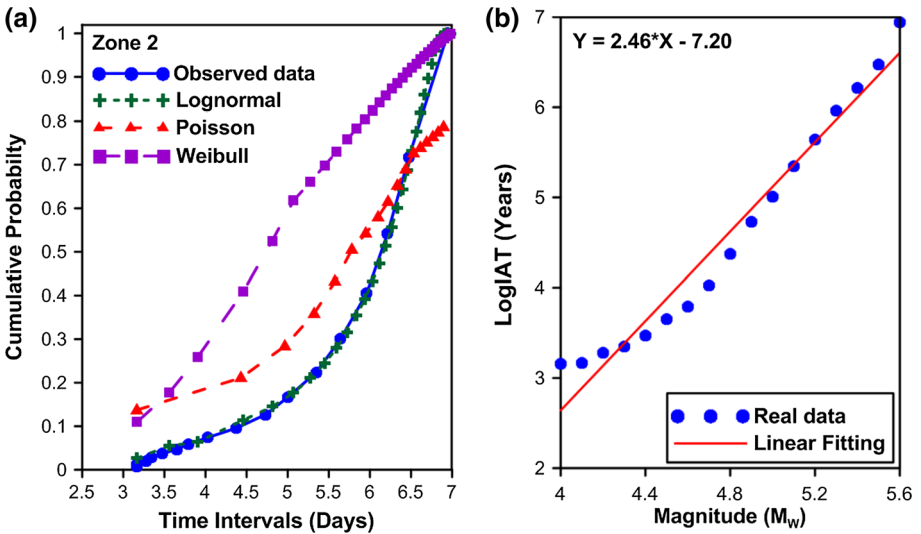


Fig. 4 a, b Same as Fig. 3a, b but for Zone 2

inter-arrival times, when the estimated p values of the test are over or equal to 0.05, i.e., the significance level $\alpha \geq 0.05$.

The term N (number of earthquakes per year exceeding magnitude M) in the Gutenberg–Richter (G–R) relationship ($\log N = a - bM$) also has some information about the inter-arrival times, because inverse of the frequency provides the recurrence interval. However,

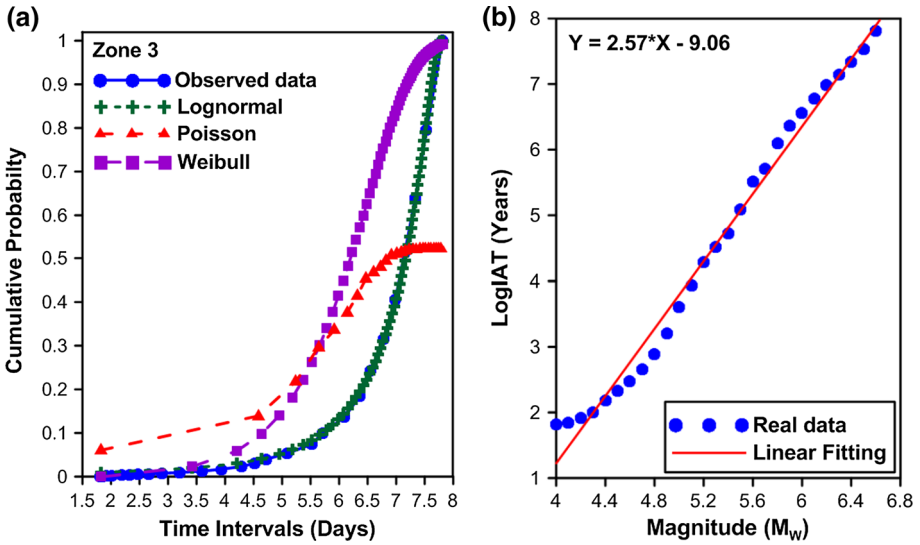


Fig. 5 a, b Same as Fig. 3a, b but for Zone 3

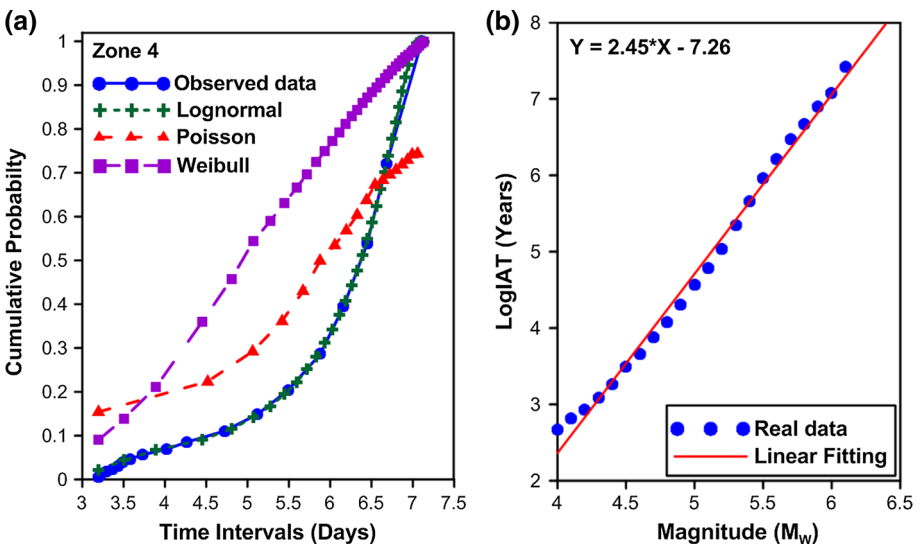


Fig. 6 a, b Same as Fig. 3a, b but for Zone 4

from G–R relation, one can interpret that the distribution of the inter-arrival times might be consistent over the whole magnitude range. Musson et al. (2002) revealed that the time-dependent seismicity Eq. (1) is more powerful than the G–R relation, albeit Eq. (1) is an alternative way of presenting G–R relation. They also confirmed that the two equations are also interrelated with each other. Thus, it is possible to calculate other measures such as median for a given mean and standard deviation of a lognormally distributed population, but the reverse of this process is not feasible. One can also determine the parameters a - and

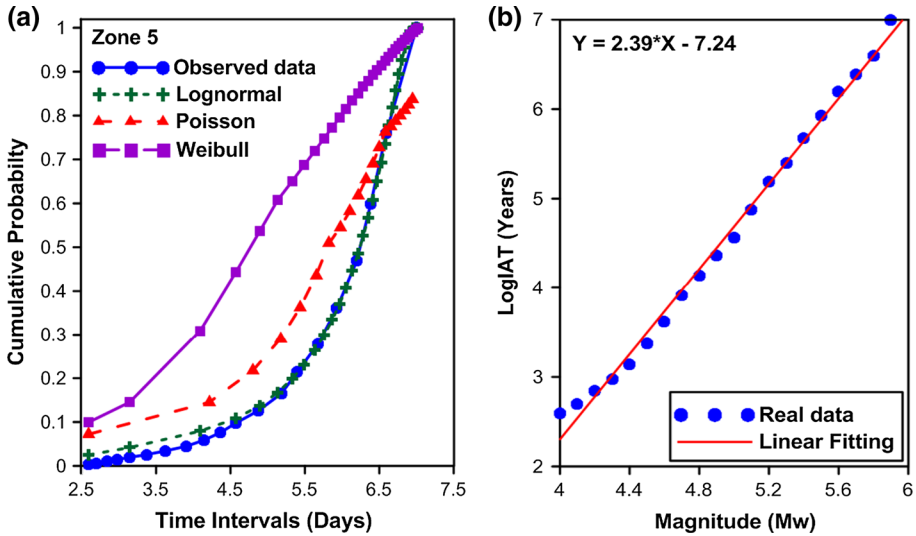


Fig. 7 a, b Same as Fig. 3a, b but for Zone 5

b -values of the G–R relation by knowing the A , B and C parameters for an earthquake population given by Eq. (1). However, it is impracticable to estimate A , B and C parameters for an earthquake population by knowing the a - and b -values from G–R relation, which implies that Eq. (1) is distinct and useful in its own right (Musson et al. 2002). Moreover, the a -value of G–R relation signifies the relative seismicity of a zone corresponding to the number of events and size of the area. This means that the a -value will be high if the seismic activity is high and the specific zone undertaken is large. Contrarily, the parameter A of Eq. (1) will be low when seismic activity is high, and thus, the average inter-arrival times decrease with the increase in seismic activity (Musson et al. 2002).

5 Results and discussion

Earthquake inter-arrival times are estimated in five main seismogenic zones of the Northwest Himalaya and adjoining regions for magnitude ranging from M_W 4.0 to the largest magnitude occurring at least twice for each zone using only the complete part of the catalogue during 1900–2010. Different models, namely Lognormal, Poisson and Weibull, are used to check the goodness of fit with the observed data (Figs. 3a, 4, 5, 6, 7a). It is observed that the estimated p values in the case of Lognormal distribution are almost equal to or more than the significance level, i.e., $\alpha \geq 0.05$, except for small magnitude, as shown in Figs. 3a, 4, 5, 6 and 7a. This implies that the Lognormal distribution fits well for practically all the data in all the zones (see Table 2). In the case of Poisson distribution, the calculated p values are more than 0.05 for lower magnitude up to M_W 4.1 but are significantly low, almost zero, for higher magnitude range in most of the zones as depicted in Table 3. This implies that the Poisson model does not give good results as it is evidenced from the p value estimation. Table 4 lists the calculated p values throughout the magnitude range in each zone for the Weibull distribution. The p values are significantly more than 0.05 for higher magnitudes starting from $M_W \geq 5.2$, while for magnitudes lower than M_W

Table 2 Results of the p values for testing the Lognormal distribution of inter-arrival times for events above any given magnitude in five zones of the studied region

Magnitude (M_w)	Zone 1	Zone 2	Zone 3	Zone 4	Zone 5
4.0	0.0020	0.0064	0.0005	0.0056	0.0029
4.1	0.0042	0.0128	0.0010	0.0113	0.0062
4.2	0.0067	0.0200	0.0016	0.0174	0.0100
4.3	0.0097	0.0277	0.0022	0.0240	0.0143
4.4	0.0133	0.0365	0.0030	0.0311	0.0194
4.5	0.0177	0.0469	0.0038	0.0385	0.0258
4.6	0.0229	0.0589	0.0048	0.0467	0.0340
4.7	0.0294	0.0742	0.0060	0.0562	0.0450
4.8	0.0374	0.0958	0.0075	0.0689	0.0588
4.9	0.0475	0.1264	0.0096	0.0850	0.0761
5.0	0.0605	0.1668	0.0126	0.1107	0.0973
5.1	0.0767	0.2238	0.0169	0.1490	0.1262
5.2	0.0974	0.3005	0.0230	0.2045	0.1655
5.3	0.1259	0.4059	0.0306	0.2862	0.2141
5.4	0.1648	0.5416	0.0400	0.3945	0.2781
5.5	0.2176	0.7176	0.0536	0.5386	0.3607
5.6	0.2849		0.0743	0.7210	0.4686
5.7	0.3726		0.0995		0.5989
5.8	0.4794		0.1365		0.7592
5.9	0.6133		0.1846		
6.0	0.7734		0.2431		
6.1			0.3160		
6.2			0.4059		
6.3			0.5117		
6.4			0.6394		
6.5			0.7948		

5.2, the p values are less than 0.05 in most of the seismogenic zones. From these inspections, we can conclude that the Lognormal distribution fits better with the data, while the Weibull model shows moderate fitting but still better than the Poisson distribution as shown in Figs. 3a, 4, 5, 6 and 7a. Similar observations have also been observed by several authors (Shimazaki et al. 1999; Musson et al. 2002 among others) during recent statistical studies of large earthquakes. Further, we investigated the correlation between the lower-bound magnitude (M_{min}), and the mean and standard deviation of the inter-arrival times using the Lognormal model for the time-dependent seismic hazard analysis.

It has been observed that all zones exhibit a good linearity between lower-bound magnitude (M_{min}) and the mean of the inter-arrival times, without any scatter at high magnitude end from the relationship. Figures 3b, 4, 5, 6 and 7b depict that the Zone 1, Zone 2, Zone 3, Zone 4 and Zone 5 show a good linear plot of log of inter-arrival time with respect to the magnitude up to magnitude M_w 6.0, 5.5, 6.5, 5.6 and 5.8, respectively. The parameters A and B are evaluated from mean of log of inter-arrival times and magnitudes by using Eq. (1). The parameter A for Zone 1, Zone 2, Zone 3, Zone 4 and Zone 5 is -7.01 (± 0.23), -7.20 (± 0.59), -9.06 (± 0.30), -7.26 (± 0.80) and -7.24 (± 0.21), respectively,

Table 3 Results of the p values for testing the Poisson distribution of inter-arrival times for events above any given magnitude in five zones of the studied region

Magnitude (M_w)	Zone 1	Zone 2	Zone 3	Zone 4	Zone 5
4.0	0.7358	0.7358	0.7358	0.7358	0.7358
4.1	0.5285	0.5285	0.5285	0.5285	0.5285
4.2	0	0	0	0	0
4.3	0	0	0	0	0
4.4	0	0	0	0	0
4.5	0	0	0	0	0
4.6	0	0	0	0	0
4.7	0	0	0	0	0
4.8	0	0	0	0	0
4.9	0	0	0	0	0
5.0	0	0	0	0	0
5.1	0	0	0	0	0
5.2	0	0	0	0	0
5.3	0	0	0	0	0
5.4	0	0	0	0	0
5.5	0	0	0	0	0
5.6	0		0	0	0
5.7	0		0		0
5.8	0		0		0
5.9	0		0		
6.0	0		0		
6.1			0		
6.2			0		
6.3			0		
6.4			0		
6.5			0		

while parameter B is 2.34 (± 0.04), 2.46 (± 0.12), 2.57 (± 0.05), 2.45 (± 0.16) and 2.39 (± 0.04), respectively. The standard deviations associated with these models are found to be 0.31, 0.23, 0.38, 0.26 and 0.21, respectively, for Zone 1, Zone 2, Zone 3, Zone 4 and Zone 5, as shown in Table 5. It is observed that the standard deviations are zone dependent, like A and B parameters of Eq. (1), and have values comparatively less than the standard deviation determined by Musson et al. (2002). At the same time, the low value of parameter A obtained from Eq. (1) depicts low average inter-arrival time for each magnitude in all the zones. Conversely, the parameters a - and b -values of the frequency-magnitude distribution (FMD) given by G–R relation are also determined for each of the five zones. In Zone 1, Zone 2, Zone 3, Zone 4 and Zone 5, the a -value is 6.58 (± 0.13), 7.85 (± 0.24), 8.60 (± 0.11), 7.29 (± 0.15) and 6.99 (± 0.15), respectively, whereas b -value is found to be 0.92 (± 0.03), 1.22 (± 0.07), 1.21 (± 0.22), 1.04 (± 0.03) and 1.01 (± 0.03), respectively (Table 6; Fig. 8a–e). It is observed that the estimated low a -values in Zone 1 and high a -values in Zone 3 obtained from the G–R relation correspond to the high and low values of A parameter in the same zones calculated from Eq. (1). This confirms the inverse relationship of Musson et al. (2002) time-dependent seismicity model’s parameter (A) with the G–R relation parameter (a -value). This reveals that the seismic activity is highest (i.e.,

Table 4 Results of the p values for testing the Weibull distribution of inter-arrival times for events above any given magnitude in five zones of the studied region

Magnitude (M_w)	Zone 1	Zone 2	Zone 3	Zone 4	Zone 5
4.0	0.0027	0.0223	0.0003	0.0148	0.0123
4.1	0.0029	0.0223	0.0003	0.0152	0.0130
4.2	0.0031	0.0245	0.0003	0.0161	0.0140
4.3	0.0034	0.0260	0.0003	0.0173	0.0151
4.4	0.0044	0.0289	0.0004	0.0182	0.0167
4.5	0.0058	0.0337	0.0004	0.0192	0.0213
4.6	0.0072	0.0382	0.0004	0.0209	0.0276
4.7	0.0092	0.0491	0.0005	0.0239	0.0372
4.8	0.0117	0.0727	0.0006	0.0327	0.0479
4.9	0.0168	0.1108	0.0008	0.0438	0.0632
5.0	0.0241	0.1569	0.0013	0.0783	0.0803
5.1	0.0344	0.2443	0.0022	0.1333	0.1198
5.2	0.0510	0.3602	0.0038	0.2222	0.1802
5.3	0.0845	0.5465	0.0059	0.3778	0.2386
5.4	0.1406	0.7590	0.0085	0.5564	0.3458
5.5	0.2294	0.9375	0.0170	0.8188	0.4859
5.6	0.3384		0.0385	0.8798	0.6930
5.7	0.5099		0.0562		0.8885
5.8	0.6867		0.1176		0.837
5.9	0.9571		0.1943		
6.0	0.7688		0.2774		
6.1			0.4101		
6.2			0.5853		
6.3			0.7624		
6.4			0.9800		
6.5			0.6409		

Table 5 The estimated values of the parameters for Eq. (1), calculated for all five zones of the studied region

Source zones	Parameter A	Parameter B	C
Zone 1	-7.01 (± 0.23)	2.34 (± 0.04)	0.31
Zone 2	-7.20 (± 0.59)	2.46 (± 0.12)	0.23
Zone 3	-9.06 (± 0.30)	2.57 (± 0.05)	0.38
Zone 4	-7.26 (± 0.80)	2.45 (± 0.16)	0.26
Zone 5	-7.24 (± 0.21)	2.39 (± 0.04)	0.21

Table 6 The estimated parameters from the G–R relationship in all five zones of the studied region

Source zones	a -value	b -value
Zone 1	6.58 (± 0.13)	0.92 (± 0.03)
Zone 2	7.85 (± 0.24)	1.22 (± 0.07)
Zone 3	8.60 (± 0.11)	1.21 (± 0.02)
Zone 4	7.29 (± 0.15)	1.04 (± 0.03)
Zone 5	6.99 (± 0.15)	1.01 (± 0.03)

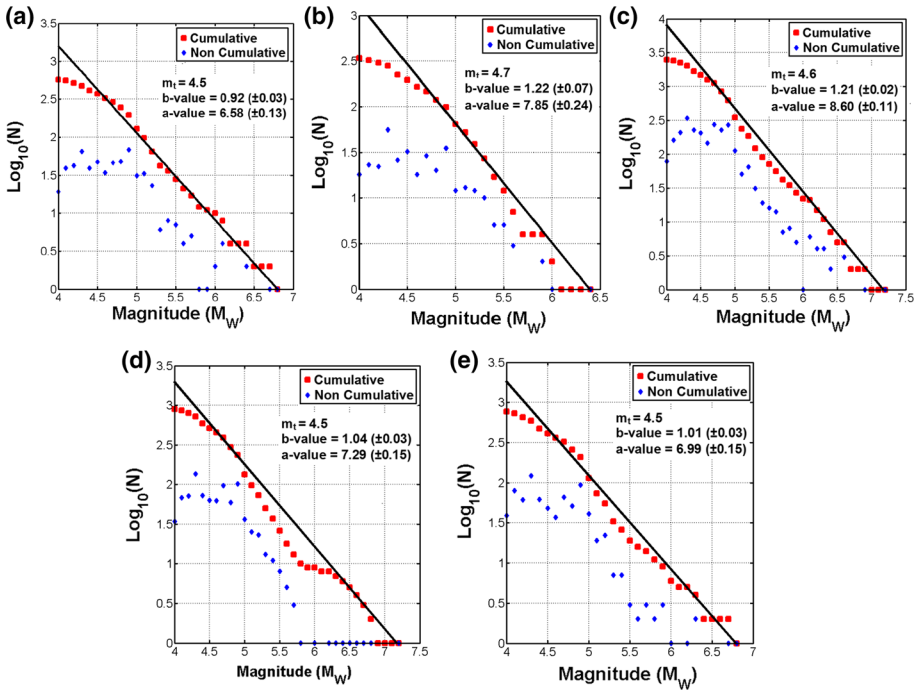


Fig. 8 Frequency–magnitude recurrence relationship in all the five zones (a–e) of the Northwest Himalaya and its adjoining regions estimated using ‘Entire Magnitude Range (EMR)’ method

low A value of -9.06 in Zone 3 (Hindukush–Pamir Himalaya) and lowest (i.e., high A value of -7.01) in Zone 1 (Sulaiman–Kirthar ranges), hence corresponding highest and lowest seismic hazard levels in these zones, respectively. This also indicates low and high recurrence periods of larger earthquakes in Zone 3 and Zone 1, respectively. Yadav et al. (2013a) also observed similar results of higher hazard level in Zone 3 as compared to Zone 1 in terms of seismic activity rate. Next higher seismic activity (i.e., lower A value of -7.26) is obtained in Zone 4 (Himalayan Frontal Thrust belt), which reveals lower recurrence periods of larger earthquakes as compared to Zone 3 of Hindukush–Pamir Himalaya. Other two zones (Zone 2 of Northern Pakistan and Hazara syntaxis and Zone 5 of Tibetan Plateau) show moderate levels of seismic activity and recurrence periods for larger earthquakes.

The results of the present study are quite consistent with that carried out in Greece and Japan by Musson et al. (2002) and suggest that the time-dependent seismicity model works well in the Northwest Himalaya and adjoining regions. Papazachos et al. (1997) applied the regional time and magnitude model for 149 seismogenic regions in the Alpine–Himalayan seismic belt and observed that the present model fits well with the seismicity in the studied region. Time-dependent seismicity was also studied by Parvez and Ram (1997) in the Hindukush Himalaya region using four statistical models (Exponential, Weibull, Gamma and Lognormal), and they also concluded that the Lognormal model fits well in the studied region. Later, Parvez and Ram (1999) applied the same statistical models for the whole Indian subcontinent and estimated time-dependent seismicity. Gumbel statistical model was applied by Shanker et al. (2007) for the three main zones (Pakistan, Hindukush and

India–Tibet) for analyzing time-dependent seismicity in the studied region. Yadav et al. (2010a) applied regional time- and magnitude-predictable model in the sixteen seismogenic zones in the Hindukush–Pamir Himalaya region. They concluded that the time-predictable model works well in this region in comparison with the slip-predictable model. An analysis of the time-dependent seismicity in the Northwest Himalaya and adjoining regions has been carried out by Yadav et al. (2012a, b, 2013a, b, 2015) using Kijko–Sellevoll method, Gumbel III distribution and Bayesian statistics. The estimated seismicity parameters (a - and b -values of G–R relation) in these previous studies match well with the present study. Yadav et al. (2012a, b, 2013a, b) also observed high and low return periods (recurrence periods) in Zone 1 (Sulaiman–Kirthar ranges) and Zone 3 (Hindukush–Pamir Himalaya), respectively, which validates the results of the present study.

6 Conclusions

The study shows that the seismicity analysis in the region can be effectively modeled as being time dependent. In this study, we used complete part of the catalogue and estimated the inter-arrival times for magnitude ranging from M_w 4.0 to the largest magnitude occurring at least twice for each zone. Fitness of the inter-arrival times is checked using the estimated p values of both K–S and Chi-square tests based on the significance level ($\alpha \geq 0.05$), which shows that the Lognormal distribution fits remarkably well and better with the inter-arrival data as compared to the Poisson and Weibull distributions. The mean of the Lognormal distribution of inter-arrival times is found to be linearly related with the lower-bound magnitude (M_{\min}). The slope (B parameter of the model) of the mean is determined and shows variation from 2.34 to 2.57. The parameter A of the applied time-dependent model shows variation between -7.01 and -9.06 in all the five seismogenic zones with corresponding lower a -value of G–R relation and lower average inter-arrival times. It is confirmed that the estimated parameter A , obtained from Musson et al. (2002) time-dependent model, has an inverse relationship with the calculated a -value from the G–R equation. It has been observed that the estimated results exhibit that the Hindukush–Pamir Himalaya (Zone 3) and Himalayan Frontal Thrust (Zone 4) have the highest earthquake hazard level and low recurrence periods as compared to other zones. This suggests that these two zones are seismically vulnerable zones in the Northwest Himalaya region. On the contrary, the Sulaiman–Kirthar ranges (Zone 1) show lowest hazard in terms of seismic activity and recurrence periods of larger earthquakes.

The present methodology can primarily be adopted in a seismogenic region for estimating the future time interval of range of magnitudes. Moreover, for any defined area, we can easily obtain the probability of an earthquake above a given magnitude as a function of time. A more detail investigation can be done on full probabilistic seismic hazard analysis by treating the whole scope of seismicity as time dependent.

Acknowledgments Authors are thankful to their respective institute/organization for necessary support to carry out this research. The first author is thankful to Secretary, Ministry of Earth Sciences, for providing necessary facilities for carrying out this work and permission to publish this paper. Authors are also thankful to two anonymous reviewers for their constructive comments and suggestions which enhanced quality of the manuscript. The GMT system (Wessel and Smith 1995) was used to plot Figs. 1 and 2.

References

- Anagnos T, Kiremidjian AS (1988) A review of earthquake occurrence models for seismic hazard analysis. *J Probab Eng Mech* 3:3–11
- Arora BR, Gahalaut VK, Kumar N (2012) Structural control on along-strike variation in the seismicity of the Northwest Himalaya. *J Asian Earth Sci* 57:15–24
- Bapat A, Kulkarni RC, Guha SK (1983) Catalogue of earthquakes in India and neighborhood from historical period up to 1979. I.S.E.T (Publ), pp 1–211
- Bufe CG, Harsh PW, Buford RO (1977) Steady-state seismic slip—a precise recurrence model. *Geophys Res Lett* 4:91–94
- Burtman V, Molnar P (1993) Geological and geophysical evidence of deep subduction of continental crust beneath the Pamir. *Geol Soc Am Spec Pap* 281:1–76
- Chandra U (1978) Seismicity, earthquake mechanisms and tectonics along the Himalayan mountain range and vicinity. *Phys Earth Planet Inter* 16:109–131
- Chatelain JL, Roecker SW, Hatzfeld D, Molnar P (1980) Micro-earthquake seismicity and fault plane solutions in the Hindukush region and their tectonic implications. *J Geophys Res* 85:1365–1387
- Chingtham P, Chopra S, Baskoutas I, Bansal BK (2013) An assessment of seismicity parameters in northwest Himalaya and adjoining regions. *Nat Hazards* 71(3):1599–1616
- Cramer CH, Petersen MD, Cao T, Topozada TR, Reichle M (2000) A time-dependent probabilistic seismic-hazard model for California. *Bull Seismol Soc Am* 90(1):1–21
- Davis PM, Jackson DD, Kagan YY (1989) The longer it has been since the last earthquake, the longer the expected time till the next? *Bull Seismol Soc Am* 79:1439–1456
- Erdik M, Demircioglu M, Sesetyan K, Durukal E, Siyahi B (2004) Earthquake hazard in Marmara region, Turkey. *Soil Dyn Earthq Eng* 24:605–631
- Fan G, Ni JF, Wallace TC (1994) Active tectonics of the Pamir and the Karakoram. *J Geophys Res* 99:7131–7160
- Frankel AD, Petersen MD, Muller CS, Haller KM, Wheeler RL, Leyendecker EV, Wesson RL, Harmsen SC, Cramer CH, Perkins DM, Rukstales KS (2002) Documentation for the 2002 update of the national seismic hazard maps. *US Geol Surv Open File Rept* 2–420
- Gansser A (1964) *Geology of the Himalayas*. Inter-Science, London
- Gardner JK, Knopoff L (1974) Is the sequence of earthquakes in southern California, with aftershocks removed, Poissonian? *Bull Seismol Soc Am* 64:1363–1367
- Goes SDB, Ward SN (1994) Synthetic seismicity for the San Andreas fault. *Ann Geof* 37:1495–1513
- Gutenberg B, Richter CF (1954) *Seismicity of the earth and associated phenomena*. Princeton University Press, New Jersey, p 310
- Kagan YY, Jackson DD (1991) Long-term earthquake clustering. *Geophys J Int* 104:117–133
- Kagan Y, Knopoff L (1976) Statistical search for non-random features of the seismicity of strong earthquakes. *Phys Earth Planet Inter* 12:291–318
- Kijko A (2004) Estimation of the maximum earthquake magnitude M_{\max} . *Pure appl Geophys* 161:1–27
- Kijko A, Sellevoll MA (1989) Estimation of seismic hazard parameters from incomplete data files part I: utilization of extreme and complete catalogues with different threshold magnitudes. *Bull Seismol Soc Am* 79:645–654
- Kijko A, Sellevoll MA (1992) Estimation of earthquake hazard parameters from incomplete data files part II: incorporation of magnitude heterogeneity. *Bull Seismol Soc Am* 82(1):120–134
- Knopoff L, Levshina T, Keilis-Borok VI, Mattoni C (1996) Increased long-range intermediate-magnitude earthquake activity prior to strong earthquakes in California. *J Geophys Res* 101:5779–5796
- Koulakov I, Sobolev S (2006) A tomographic image of Indian lithosphere break-off beneath the Pamir-Hindukush region. *Geophys J Int* 164:425–440
- Kumamoto T (1999) Seismic hazard maps of Japan and computational differences in models and parameters. *Geograph Rev Jpn Ser B* 72(2):135–161
- Meltzer A, Sarker G, Beaudoin B, Seeber L, Armbruster J (2001) Seismic characterization of an active metamorphic massif, Nanga Parbat, Pakistan Himalaya. *Geology* 29:651–654
- Mulgaria F, Tinti S (1985) Seismic sample areas defined from incomplete catalogs: an application to the Italian territory. *Phys Earth Planet Inter* 40(4):273–300
- Musson RMW, Tsapanos T, Nakas CT (2002) A power-law function for earthquake interarrival time and magnitude. *Bull Seismol Soc Am* 92:1783–1794
- Oldham T (1883) A catalogue of Indian earthquakes from the earliest time to the end of A.D. 1869. *Mem Geol Surv India* 19(3):53
- Pace B, Perruzza L, Lavecchia G, Bancio P (2006) Layered seismogenic source model and probabilistic seismic-hazard analyses in central Italy. *Bull Seismol Soc Am* 96:107–132

- Papadimitriou EE, Papazachos BC (1994) Time dependent seismicity in the Indonesian region. *J Geophys Res* 99:15387–15398
- Papaoiannou C, Papazachos C (2000) Time-independent and time-dependent seismic hazard in Greece based on seismogenic sources. *Bull Seismol Soc Am* 90:22–33
- Papazachos BC (1989) A time predictable model for earthquake generation in Greece. *Bull Seismol Soc Am* 79:77–84
- Papazachos BC (1992) A time and magnitude predictable model for generation of shallow earthquakes in the Aegean area. *Pure appl Geophys* 138:287–308
- Papazachos BC, Papaioannou ChA (1993) Long term earthquake prediction in Aegean area based on a time and magnitude predictable model. *Pure appl Geophys* 140:593–612
- Papazachos BC, Papadimitriou EE, Karakaisis GF, Tsapanos TM (1994) An application of the time- and magnitude-predictable model for the long-term earthquake prediction of strong shallow earthquakes in the Japan area. *Bull Seismol Soc Am* 84:426–437
- Papazachos BC, Karakaisis GF, Papadimitriou EE, Papaioannou ChA (1997) The regional time and magnitude-predictable model and its application to the Alpine–Himalayan belt. *Tectonophysics* 271:295–323
- Parvez IA, Ram A (1997) Probabilistic assessment of earthquake hazards in the north-east Indian peninsula and Hindukush regions. *Pure appl Geophys* 149:731–746
- Parvez IA, Ram A (1999) Probabilistic assessment of earthquake hazards in the Indian subcontinent. *Pure appl Geophys* 154:23–40
- Peruzza L, Pace B (2002) Sensitivity analysis for seismic source characteristics to probabilistic seismic hazard assessment in central Appennines (Abruzzo area). *Boll di Geofisica Teorica ed Applicata* 43:79–100
- Petersen MD, Cao T, Campbell KW, Frankel AD (2007) Time-independent and time-dependent seismic hazard assessment for the state of California: Uniform California Earthquake rupture forecast model 10. *Seismol Res Lett* 78(1):99–109
- Petersen MD, Frankel AD, Harmsen SC, Mueller CS, Haller KM, Wheeler RL, Wesson RL, Zeng Y, Boyd OS, Perkins DM, Luco N, Field EH, Wills CJ, Ruksatles KS (2008) Documentation for the 2008 update of the United States national seismic hazard maps. *US Geol Surv Open File Rept* 2008–1128:60
- Quittmeyer RC, Jacob KH (1979) Historical and modern seismicity of Pakistan, Afghanistan, northern India, and southern Iran. *Bull Seismol Soc Am* 69:773–823
- Reid HF (1911) The elastic-rebound theory of earthquakes. *Univ Calif Pub Bull Dept Geol* 6:413–444
- Seeber L, Armbruster JG (1981) Great detachment earthquakes along the Himalayan arc and long forecasting: In: Richards DW, Simpson PG (eds) *Earthquake prediction—an international review*, Maurice Ewing Series. American Geophysical Union, vol 4, pp 259–277
- Shanker D, Yadav RBS, Singh HN (2007) On the seismic risk in the Hindukush–Pamir Himalaya and their vicinity. *Curr Sci* 92:1625–1630
- Shimazaki K, Nakata T (1980) Time predictable recurrence of large earthquakes. *Geophys Res Lett* 7:279–282
- Shimazaki K, Kawase K, Satake K, Suzuki Y, Ogata Y, Imoto M, Kumamoto T (1999) Renewal recurrence models for large earthquakes in Japan. *IUGG99 Abstracts* 2:B182
- Sornette D, Knopoff L (1997) The paradox of the expected time until the next earthquake. *Bull Seismol Soc Am* 87:789–798
- Sykes LR, Quittmeyer RC (1981) Repeat times of great earthquakes along simple plate boundaries. In: *Earthquake prediction, an international review*, Maurice Ewing Series. American Geophysical Union, vol 4, pp 217–247
- Tandon AN, Srivastava HN (1974) Earthquake occurrences in India. *Earthquake Engineering*, Jai Krishna Volume, Sarita Prakashan (publ), pp 1–48
- Thingbaijam KKS, Chingtham P, Nath SK (2009) Seismicity in the north–west Frontier Province at the Indian–Eurasian plate convergence. *Seismol Res Lett* 80(4):599–608
- Tripathi JN (2006) Probabilistic assessment of earthquake recurrence in the January 26 2001 earthquake region of Gujarat India. *J Seismol* 10:119–130
- Tsapanos TM, Papazachos BC (1994) Long term earthquake prediction in China based on the time and magnitude predictable model. *J Earthq Pred Res* 3:237–256
- Uhrhammer RA (1986) Characteristics of northern and central California seismicity. *Earthquake Notes* 57(1):21 (**abstract**)
- Ward SN, Goes SDB (1993) How regularly do earthquakes recur? A synthetic seismicity model for the San Andreas fault. *Geophys Res Lett* 20:2131–2134
- Wessel P, Smith WHF (1995) New version of the generic mapping tools released. *EOS Trans Am Geophys Union* 76:329

- Working Group on California Earthquake Probabilities (WGCEP) (1995) Seismic hazards in southern California: probable earthquakes, 1994 to 2024. *Bull Seismol Soc Am* 85:379–439
- Working Group on California Earthquake Probabilities (WGCEP) (2003) Earthquake Probabilities in the San Francisco Bay region: 2000 to 2030. *US Geol Surv Circ* 1189
- Yadav RBS (2009) Seismotectonic modeling of NW Himalaya: a perspective on future seismic hazard. Ph.D. Thesis, Department of Earthquake Engineering, IIT Roorkee, India
- Yadav RBS, Tripathi JN, Rastogi BK, Chopra S (2008) Probabilistic assessment of earthquake hazard in Gujarat and adjoining region of India. *Pure appl Geophys* 165:1813–1833
- Yadav RBS, Shanker D, Chopra S, Singh AP (2010a) An application of regional time and magnitude predictable model for long-term earthquake prediction in the vicinity of October 8 2005 Kashmir Himalaya earthquake. *Nat Hazards* 54(3):985–1014
- Yadav RBS, Tripathi JN, Rastogi BK, Das MC, Chopra S (2010b) Probabilistic assessment of earthquake recurrence in Northeast India and adjoining region. *Pure appl Geophys* 167(11):1331–1342
- Yadav RBS, Bayrak Y, Tripathi JN, Chopra S, Singh AP, Bayrak E (2012a) A probabilistic assessment of earthquake hazard parameters in NW Himalaya and the adjoining regions. *Pure appl Geophys* 169:1619–1639
- Yadav RBS, Bayrak Y, Tripathi JN Chopra, Bayrak SE (2012b) Regional variation of the x-upper bound magnitude of GIII distribution in Hindukush–Pamir Himalaya and the adjacent regions: a perspective on earthquake hazard. *Tectonophysics* 544–545:1–12
- Yadav RBS, Tsapanos TM, Bayrak Y, Koravos GCH (2013a) Probabilistic appraisal of earthquake hazard parameters deduced from a Bayesian approach in the northwest frontier of the Himalayas. *Pure appl Geophys* 170(3):283–295
- Yadav RBS, Tsapanos TM, Koravos GCH, Bayrak Y, Devlioti KD (2013b) Spatial Mapping of Earthquake Hazard Parameters in the Hindukush–Pamir Himalaya and adjacent regions: a perspective on future hazard. *J Asian Earth Sci* 70:115–124
- Yadav RBS, Koravos GCH, Tsapanos TM, Vougiouka EG (2015) A probabilistic estimate of most perceptible earthquake magnitudes in the NW Himalaya and adjoining regions. *Pure appl Geophys* 172(2):197–212